

# CHARACTERIZATION OF TEMPORAL BIODEGRADATION OF RADIATA PINE BY *GLOEOPHYLLUM TRABEUM* THROUGH PRINCIPAL COMPONENT ANALYSIS-BASED TWO-DIMENSIONAL CORRELATION FTIR SPECTROSCOPY

CLAUDIO POZO<sup>1</sup>, JUDITH DÍAZ-VISURRAGA<sup>1</sup>, DAVID CONTRERAS<sup>2,4</sup>,  
JUANITA FREER<sup>2,4</sup>, JAIME RODRÍGUEZ<sup>2,3</sup>

<sup>1</sup>Centro de Investigación de Polímeros Avanzados (CIPA) CONICYT- REGIONAL R08C1002. Av. Collao N°1202 Edificio Lab. CIPA, Concepción, Chile

<sup>2</sup>Centro de Biotecnología, Universidad de Concepción. Barrio Universitario s/n, Casilla 160-C, Concepción, Chile

<sup>3</sup>Facultad de Ciencias Forestales, Universidad de Concepción. Victoria 631, Casilla 160-C, Concepción, Chile

<sup>4</sup>Facultad de Ciencias Químicas, Universidad de Concepción. Edmundo Larenas 129, Casilla 160-C, Concepción, Chile

## ABSTRACT

Brown rot fungi produce a special pattern of wood decay. In the first stages of biodegradation, fast depolymerisation of holocellulose causes a rapid loss of wood strength while lignin is not substantially depolymerized. Fourier Transform Infrared Spectroscopy (FTIR) is a powerful tool for examining changes in wood chemistry. FTIR is an accurate, non-destructive technique, which usually requires a minimum of sample preparation and sample size. Principal component analysis-based two-dimensional (PCA2D) correlation spectroscopy of a spectral data set was applied to assess temporal brown-rot wood decay. *Pinus radiata* with soil support was degraded by brown rot fungi *Gloeophyllum trabeum* for a period of 0, 1, 2, 3, 4, 8, 12 and 16 weeks simulating the natural process of biodegradation. Decayed samples were monitored and analyzed periodically by FTIR. Most of the autopeaks had contributions from lignin, cellulose, and hemicelluloses. The main effect observed by PCA2D correlation was the significant decrease in the intensities of bands predominantly in the region of 2000-1000 cm<sup>-1</sup>, associated with polysaccharides in the biodegraded wood. An increase in the intensities of bands at 1698 and 1664 cm<sup>-1</sup> associated with the oxidation of wood components, mostly lignin, was also observed. Detailed analysis of asynchronous map showed that the wood oxidation began after the depolymerisation of polysaccharides.

**Keywords:** FTIR-PCA2D correlation spectroscopy, Brown rot, *Gloeophyllum trabeum*.

## 1. INTRODUCTION

Brown rot fungi produce a special pattern of wood decay characterized by the oxidative degradation of wood cell wall components causing a rapid loss of wood strength<sup>1</sup>. The degradation mechanism is based on iron reducing compounds of low molar mass which promote Fenton reactions<sup>2-7</sup>.

The Fenton reaction ( $\text{Fe(II)} + \text{H}_2\text{O}_2 \rightarrow \text{Fe(III)} + \text{OH}^- + \bullet\text{OH}$ ) generates hydroxyl radicals from hydrogen peroxide which oxidize organic molecules<sup>3, 8</sup>. Low molar mass dihydroxybenzenes (DHBs) and demethylated lignin, produced during brown rot degradation of wood, promote Fenton reactions by iron chelation and reduction<sup>9</sup>. The first biodegradation stage consists of holocellulose depolymerisation<sup>10</sup>. Brown rot fungi always remove hemicelluloses prior to amorphous and crystalline cellulose<sup>1</sup> and modify lignin through a demethylations process<sup>11, 12</sup>. They also oxidize lignin side chains to a lesser extent without substantial depolymerisation<sup>13</sup>.

Fourier transform infrared (FTIR) spectroscopy is a powerful tool for characterizing lignocellulosics and for examining changes in wood chemistry of materials subjected to chemical treatments and different environmental conditions<sup>14</sup>. This technique is accurate, non-destructive and usually requires a minimum of sample preparation and sample size. Only few milligrams are required compared with conventional gravimetric techniques where several grams are required. Studies of fungal wood decay using mid infrared (MIR) techniques have been developed by several authors<sup>15-18</sup>.

Two-dimensional correlation spectroscopy (2DCOS) is a technique for evaluating the relationships among different functional groups in the molecules<sup>19</sup>. The concept has evolved into the so-called generalized two-dimensional correlation spectroscopy for the detailed analysis of various spectral data<sup>20</sup>. The construction of 2DCOS is based on the detection of dynamic changes of a system under an external perturbation. Perturbation methods can include both static (e.g., temperature, composition, pressure and stress, spatial distribution and orientation) and dynamic types (e.g., rheo-optical and acoustic, chemical reactions and kinetics, H/D exchange, sorption and diffusion)<sup>21</sup>. 2DCOS has been employed in the study of wood biodegradation by soft rot fungi<sup>22</sup>.

2DCOS consists of two kinds of spectra, a synchronous and asynchronous map. The former represents coupled or related changes in spectral intensity, while the latter represents independent spectral variations<sup>19, 20</sup>. The positive or negative signs of the synchronous and asynchronous correlation peaks can help to identify the sequence of the responses of various components induced

by a specific external stimulus applied to the system<sup>20</sup>. 2DCOS, including synchronous and asynchronous map, has been certainly one of the most sensitive techniques for interpreting spectral data sets obtained during the observation of a system under some external perturbation<sup>23</sup>. However, for very noisy spectra it is difficult to separate completely the real signals from noise in 2D correlation spectra.

Principal component analysis-based two-dimensional (PCA2D) correlation spectroscopy is one of the most effective methods to improve the data quality for 2D correlation analysis. This processing implies a great advantage in terms of noise suppression for the generalized 2DCOS<sup>24</sup>.

In this work, PCA2D correlation spectroscopy was applied to the analysis of the chemical changes occurring in brown-rotted wood (BRW), considering the spectral features observed as the result of the perturbation produced by the temporal wood biodegradation.

## 2. EXPERIMENTAL

### 2.1 Chemicals

Nanopure water (NPW) was used in all experiments and analyses. Soy protein acid hydrolysate (Sigma); Agar-agar for microbiology (Merck); Malt extract for microbiology (Merck) were used for culture medium. Potassium bromide (Merck) for IR spectroscopy was employed for FTIR characterization. For chemical analysis (unless otherwise stated, all reagents were p.a. grade): Sodium chloride 80% (Fluka); Copper(II) ethylenediamine solution (Merck); Sulphuric acid 98% (Merck); Acetone 99% (Merck).

### 2.2 Fungus inoculum preparation

Wood chips (heartwood and sapwood mixtures) were incubated on soil for 0, 1, 2, 3, 4, 8, 12 and 16 weeks. All the experiments were carried out in triplicate. It is noteworthy that the amount of heartwood is negligible in this wood.

Wood of radiata pine trees (20 year old) was chipped and screened to approximately 2.0 cm×2.5 cm×0.5 cm. The wood chips were immersed in water for 24 h, and then the residual water was drained off before autoclaving for 20 minutes at 121°C.

A stationary tray bioreactor, consisting of a 30 cm (length) x 20 cm (width) x 7 cm (height) plastic tray, was used in this experiment according to the method proposed by Akhtar et al. (1992)<sup>25</sup>. Two hundred fifty cm<sup>3</sup> of sieved

soil (mesh 5), obtained from the forest reserves in Concepcion, Chile (36° 50' 29'' S, 73° 1' 33'' O), was autoclaved for 20 min at 121 °C. Three hundred g (on dry basis) of autoclaved chips were put in the tray bioreactor along with the soil.

Materials were autoclaved separately in order to avoid the diffusion of metals from soil to wood. The final moisture of wood was 60% and 37% for soil.

*Gloeophyllum trabeum* (ATCC 11539) cultures were maintained in water at 4 °C and then grown on agar-agar plates for 7 days at 25 °C. Erlenmeyer flasks containing 200 mL of nutritive medium (2% malt extract and 0.5% soy protein) were inoculated with 20 discs (8 mm diameter) cut from the *G. trabeum* culture. These liquid cultures were maintained under static conditions for 15 days at 25 °C. The mycelial pellets were then removed by filtration and washed with 500 mL of sterilized water. The washed mycelia from several flasks were blended with 100 mL of sterilized water for 15 s (three cycles) and used to inoculate the wood chips.

Inoculation of wood chips was performed before putting the wood on soil. Mycelium mass/wood ratio was 1000 mg kg<sup>-1</sup> (on dry basis). Each stationary tray bioreactor was placed inside a sterile polypropylene containment bag. All cultures were incubated under static conditions at 25 °C for 0, 1, 2, 3, 4, 8, 12 and 16 weeks. At the end of each incubation period, the wood chips were separated from the soil, dried at 45 °C for 48 h and stored under dry conditions for further characterization. The mycelium on the wood surface was not removed.

From each tray approximately 75 g of chips were collected by random sampling. Each replicate (3) was pulverized using a Cyclotec 1093 sample mill (Foss NIR Systems Inc.). After that, the samples were dried at 105 °C for 1h for the spectra acquisition.

After biodegradation, the wood chips were separated from soil, dried at 45 °C for 48 h and stored in dry conditions for further characterization. The mycelium on the wood surface was not removed. Weight loss was calculated based on the initial and final dry weights. All values were corrected by weight loss except where otherwise noted.

### 2.3 Chemical analysis of the wood chips

For chemical analysis, air-dried samples were milled in a knife mill (Manesco & Ranieri) and passed through an 18 mesh. To obtain a representative sample, each sample was mixed and partitioned using a quartering method<sup>26</sup>. Approximately 1 g of sample was extracted with 99% acetone for 16 h in a Soxhlet apparatus following standard method (TAPPI Test Method T 280 pm-99).

Total lignin content was determined by the sum of Klason lignin and soluble lignin in aqueous fraction. Klason lignin was determined in extractive-free wood samples according to TAPPI Standard T 222 om-98, 1998 and TAPPI Standard T 222 om-98, 1998. Acid insoluble lignin in wood and pulp, TAPPI T222 om-98 (1998). Soluble lignin in the aqueous fraction was determined by measuring the absorbance at 205 nm and by using an absorptivity of 105 Lg<sup>-1</sup>cm<sup>-1</sup><sup>27</sup>.

Chlorite holocellulose was prepared following standard method TAPPI T-9m-54. The volume and weight used in this procedure were scaled in proportion to the mass of air-dried wood used in each preparation.

Correlation between one dimensional FTIR and chemical properties of biodegraded wood chips (percent of weight loss, total lignin and holocellulose) were obtained using Statgraphics Plus 3.1 software (Manugistics Inc., Rockville, USA).

### 2.4 FTIR and PCA2D correlation analysis

FTIR spectra were recorded in a Perkin Elmer FT-2000 FTIR spectrometer in the range of 4000-400 cm<sup>-1</sup> with a resolution of 4 cm<sup>-1</sup> using the KBr pellet technique. Background and sample spectra were obtained from 64 scans. About 25 mg of sample was ground with 275 mg of dry potassium bromide and a pellet was formed using a press at a pressure of about 103.4 MPa. All spectra were baseline corrected around the spectral regions of 3800, 1800 and 800 cm<sup>-1</sup>, offsetting to a zero absorbance value, and then normalized on the basis of the internal standard band nearest to 1510 cm<sup>-1</sup>. The three spectra of each sample

(independent triplicate) were averaged and a data matrix was created.

Prior to principal component analysis (PCA) calculations, the mean centering operation was performed on the data matrix. The 1800-800 cm<sup>-1</sup> spectral range was considered, while the rest of data were excluded from the analysis.

The PCA2D correlation spectroscopy, synchronous and asynchronous maps were calculated according to algorithms described by Noda et al<sup>23</sup> and Jung et al<sup>24</sup>. Data processing and analysis were performed using MATLAB software 7.4.0.287 R2007a (The Math Works, Inc.). PCA was performed using Pirouette software 3.11 (Infometrix Co., Tulsa, OK, USA).

According to Noda's rule<sup>23</sup> the intensity peaks located at diagonal positions  $v_1 = v_2$  of the synchronous map are called autopeaks. These peaks are always positive and appear when there are changes in the region of interest in terms of intensity under a given perturbation. The off-diagonal peaks are called crosspeaks. They reflect changes at the same time but not necessarily in the same direction of the variations of two spectral intensities measured at  $v_1$  and  $v_2$ . A positive synchronous crosspeak indicates that the variations in intensity of the two peaks at  $v_1$  and  $v_2$  proceed in the same direction during the observation period (both increases or both decreases), while a negative synchronous crosspeak of the two peaks at  $v_1$  and  $v_2$  shows that the changes are in the opposite directions (one increases, while the other one decreases). An asynchronous map has only off-diagonal peaks. In the synchronous map, the function between two wavenumbers ( $v_1/v_2$ ) is defined by  $\phi(v_1, v_2)$ , while in the asynchronous map it is defined by  $\psi(v_1, v_2)$ . According to the sequence rules proposed by Noda<sup>23</sup>, if a crosspeak in the synchronous map  $\phi(v_1, v_2) > 0$  and the crosspeak at the same position in the asynchronous map  $\psi(v_1, v_2) > 0$ , the change at  $v_1$  occurs prior to that at  $v_2$ . If the crosspeak in the asynchronous map is negative, the change at  $v_2$  occurs prior to that at  $v_1$ . The rule is inverted for  $\phi(v_1, v_2) < 0$ . All crosspeaks are represented as  $(v_1/v_2)$ .

## 3. RESULTS AND DISCUSSION

### 3.1 One dimensional FTIR analysis

Fig. 1 shows the reconstructed FTIR spectra of decayed wood measured during the degradation process over a 16-week period. The reconstructed data matrix from the three principal components was used instead of the original raw spectral data matrix for the subsequent 2D correlation analysis. PCA factor 1 (PC<sub>1</sub>), factor 2 (PC<sub>2</sub>), and factor 3 (PC<sub>3</sub>) accounted for 96.1%, 2.8%, and 1.0%, of the total variance of spectral intensities, respectively. The spectral region between 1800-800 cm<sup>-1</sup> is known as the fingerprint region of wood; this region is very complex because many bands have contributions from all components of wood (cellulose, hemicelluloses, and lignin)<sup>28, 29</sup>. All FTIR spectra were normalized at 1510 cm<sup>-1</sup> since this band is considered a 'pure' band related to the aromatic groups present in lignin<sup>15</sup>. The observed changes in the FTIR spectrum of BRW in this study were consistent with previous reports<sup>15, 17, 30</sup>. The intensity of principal bands studied within this spectral range is summarized in Table 1.

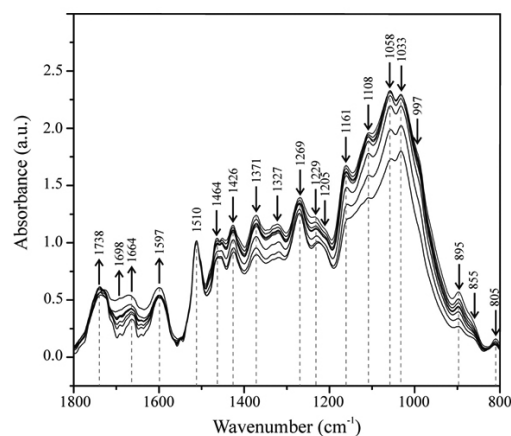


**Figure 1.** Reconstructed data of the FTIR spectra of the wood sample studied from loading vectors and scores of PC<sub>1</sub>, PC<sub>2</sub> and PC<sub>3</sub> in 1800–800 cm<sup>-1</sup>. Arrows indicate the directions of the changes in the intensity bands with increasing of biodegradation time.

**Table 1.** Assignment of principal infrared bands identified in radiata pine wood chips biotreated by *G. trabeum*.

$\nu(\text{cm}^{-1})$ range of maxima	Band position (16 week) ( $\text{cm}^{-1}$ )	Band assignment <sup>a</sup>	Principal band's origin
1709-1738	1668, 1738	C=O stretch in unconjugated ketones and in ester groups (frequently of polysaccharide origin); conjugated aldehydes and carboxylic acids absorb around and below $1700 \text{ cm}^{-1}$ <sup>29,31</sup>	Lignin/polysaccharide
1675-1655	1664	C=O stretch on conjugated <i>p</i> -substituted aryl ketones <sup>28, 29, 31</sup>	Lignin
1593-1605	1597	Aromatic skeletal vibrations plus C=O stretch <sup>28, 29, 31, 32</sup>	Lignin
1505-1515	1510	Aromatic skeletal vibration <sup>28, 29, 31, 32</sup>	Lignin
1460-1470	1464	C-H deformations; asymmetric in $-\text{CH}_3$ and $-\text{CH}_2-$ <sup>28, 29, 31</sup>	Lignin/polysaccharide
1430-1422	1426	Aromatic skeletal vibration combined with C-H in plane deformation in lignin <sup>28, 29, 31</sup> and polysaccharide <sup>17, 30</sup>	Lignin/polysaccharide
1370-1365	1371	Phenolic OH <sup>28, 29</sup> , aliphatic C-H stretch in $\text{CH}_3$ , not in O-Me <sup>28, 29, 31</sup> , C-H vibration in polysaccharide <sup>17, 30</sup>	Lignin/polysaccharide
1330-1325	1327	Phenolic OH <sup>31</sup> , S ring plus G ring condensed (i.e G ring substituted in pos. 5) <sup>28, 29, 31</sup> , C-H vibration in polysaccharide <sup>17, 30</sup>	Lignin/polysaccharide
1270-1266	1269	G ring plus C=O stretch <sup>28, 29, 31</sup> , acetyl and carboxylic vibration in xylan <sup>32</sup>	Lignin/polysaccharide
1230-1221	1229	C-C plus C-O plus C=O stretch <sup>28, 29, 31</sup> , acetyl and carboxylic vibration in xylan <sup>32</sup>	Lignin/polysaccharide
1205-1200	1205	OH in-plane bending in cellulose I and cellulose II <sup>31</sup>	Polysaccharide
1160	1161	C-O-C asymmetric stretch vibration in cellulose and hemicelluloses <sup>31</sup>	Polysaccharide
1106	1108	C-O and C-C stretching and $\text{CH}_2$ rocking in cellulose <sup>28</sup>	Polysaccharide
1060	1058	C-O stretching vibrations of cellulose and hemicelluloses <sup>31, 33</sup>	Polysaccharide
1035-1030	1033	C-O deformation in primary alcohols; plus C=O stretch (unconj.); plus aromatic C-H in-plane deformation in lignin <sup>28, 29, 31</sup> , C-O and C-C stretching and $\text{CH}_2$ rocking in cellulose <sup>28</sup>	Lignin/Polysaccharide
998	997	C-O stretching in cellulose and hemicellulose <sup>32</sup>	Polysaccharide
895-892	895	Anomere C-groups, $\text{C}_1$ -H deformation, ring valence vibration <sup>31</sup>	Polysaccharide
858-853	855	C-H out-of-plane in position 2, 5 and 6 of G units <sup>28, 29, 31</sup>	Lignin
805	805	Glucomanan <sup>34</sup>	Polysaccharide

<sup>a</sup>G: guaiacyl, S: syringyl

The observed changes in the one dimensional FTIR spectra of biodegraded wood (Fig. 1), are reflected in the decreases in bands at 1205, 1161, 1108, 1058 and  $997 \text{ cm}^{-1}$ , which are related to the strong absorption of -C-O- present in the polysaccharides <sup>15</sup>. This decrease is due to the selective consumption of polysaccharides by brown rot fungi (Fig. 4). Another effect of the biodegradation process by brown rot fungi is reduced cellulose crystallinity <sup>1</sup>. The -C-O-C- band at  $1161 \text{ cm}^{-1}$  is sensitive to changes in cellulose crystallinity, with the band decreasing with decreasing crystallinity <sup>31</sup>.

The major softwood hemicelluloses are composed of partially acetylated galactoglucomannans and a small amount of arabino-4-O-methylglucuronoxylans <sup>28</sup>. The decreases in bands at 1269 and  $1229 \text{ cm}^{-1}$  could be related to hemicelluloses biodegradation, since these bands result partially from acetyl and carboxylic vibration in xylan <sup>32</sup>.

Softwood lignin is mainly composed of guaiacyl (G) units with small amounts of syringyl (S) and only traces of *p*-hydroxyphenyl type units <sup>28</sup>. The FTIR spectrum of BRW revealed a predominance of G bands with higher intensities at 1269, 1229, and a shoulder around  $855 \text{ cm}^{-1}$ . Softwood lignin absorbs near 1269 and  $1229 \text{ cm}^{-1}$  and hardwood lignin only absorbs at  $1229 \text{ cm}^{-1}$  <sup>35</sup>. Although the content of phenolic OH in BRW tends to increase over time <sup>36</sup>, it is likely that this effect at 1371 and  $1327 \text{ cm}^{-1}$  was offset by the polysaccharide biodegradation.

The intensities of bands assigned to lignin at  $1597 \text{ cm}^{-1}$  showed an important

increase; however, the bands in the fingerprint region contained further information about lignin and polysaccharide content. Bands at 1426, 1371, 1327, 1269 and  $1229 \text{ cm}^{-1}$  revealed an important decrease in the intensities that could be mainly attributed to biodegradation of polysaccharides.

The FTIR spectrum of all BRW samples displayed bands at 1597, 1510, and  $1426 \text{ cm}^{-1}$  corresponding to the aromatic ring vibrations of the phenyl propane skeleton <sup>37</sup>, with weaker changes at  $1597 \text{ cm}^{-1}$  than carbohydrates bands (Table 1). This confirms that the "core" of the lignin structure did not change dramatically during the biodegradation process, showing a low rate of mass loss (Fig. 4). The intensity of the band at  $1426 \text{ cm}^{-1}$  decreased due to degradation of associated polysaccharides.

Bands at 1738, 1698 and  $1664 \text{ cm}^{-1}$  could be related to oxidative processes produced by brown rot fungi. The small change in intensities of the band at  $1738 \text{ cm}^{-1}$  can be explained because the changes caused by oxidation were offset by depolymerization of xylan, which absorbs at this band <sup>17</sup>.

Peaks at 1161, 1108, 1058 and  $997 \text{ cm}^{-1}$  were obviously stronger than other prominent peaks at 1738, 1698, 1664, 1464, 1426, 1371, 1327, 1229 and  $895 \text{ cm}^{-1}$  (Fig. 2). The strong peaks indicated that polysaccharides were highly susceptible to biodegradation by brown rot fungi (Fig. 4). Bands associated with C-O, C-C and C-O-C stretching vibrations of cellulose and hemicelluloses showed greater changes in intensity; this is consistent with the known wood decay pathway of brown rot fungi which preferably degrade hemicellulose and cellulose, leaving a chemically modified, depolymerised lignin residue <sup>11, 12</sup>.

### 3.2 Two dimensional FTIR correlation analysis

The range  $1800\text{--}800\text{ cm}^{-1} \times 1800\text{--}800\text{ cm}^{-1}$  was divided into four quadrants for better interpretation of the synchronous and asynchronous map. The  $1800\text{--}1200\text{ cm}^{-1} \times 1800\text{--}1200\text{ cm}^{-1}$  and  $1200\text{--}800\text{ cm}^{-1} \times 1200\text{--}800\text{ cm}^{-1}$  quadrants were used for autopeak analysis. The  $1800\text{--}1200\text{ cm}^{-1} \times 1200\text{--}800\text{ cm}^{-1}$  quadrant was used for crosspeak analysis (Fig.3). A power spectrum, corresponding to the synchronous correlation intensity along the diagonal line, illustrates the extent of the intensity changes (Fig. 2).

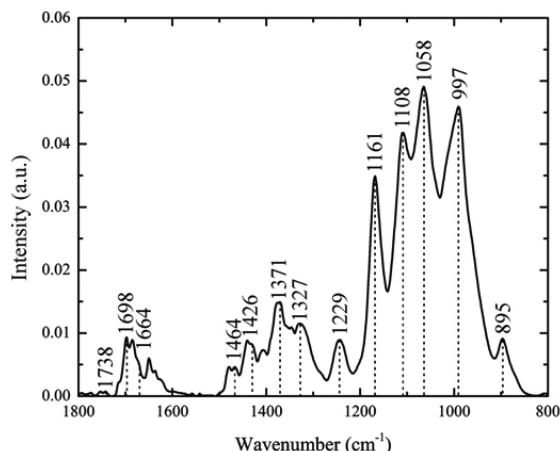


**Figure 2.** Power spectrum of BRW in the region of  $1800\text{--}800\text{ cm}^{-1}$  and main peaks.

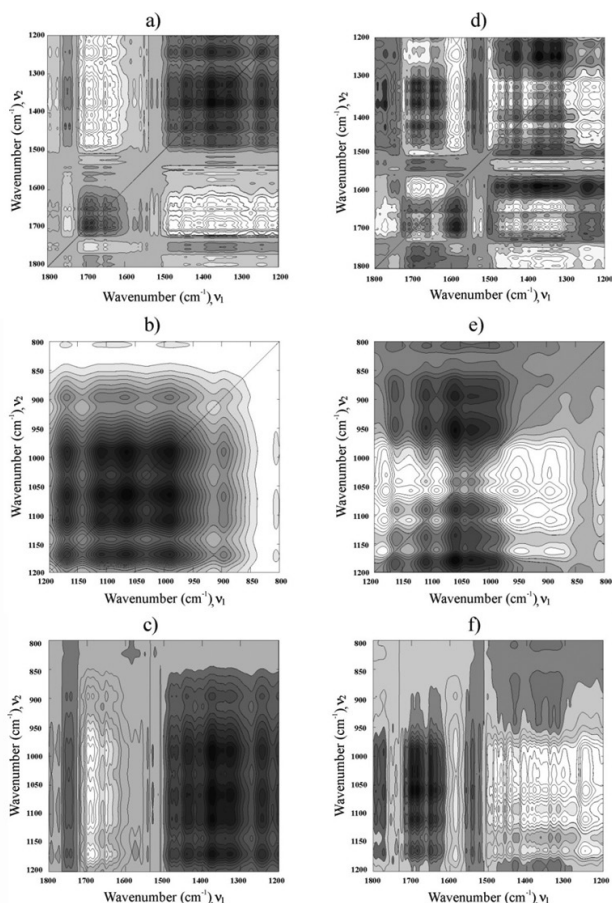


**Figure 3.** Two dimensional FTIR correlation analysis in the  $1800\text{--}800\text{ cm}^{-1} \times 1800\text{--}800\text{ cm}^{-1}$  region divided into quadrants, for synchronous (a-c) and asynchronous maps (d-f). Dark and light color represent positive and negative crosspeaks, respectively.

The synchronous map in the  $1800\text{--}1200\text{ cm}^{-1}$  region (Fig. 3a) showed seven weak autopeaks on the diagonal at approximately  $1698, 1664, 1426, 1371, 1327$  and  $1229\text{ cm}^{-1}$ . Four strong autopeaks on the diagonal at approximately  $1161, 1108, 1058, 997\text{ cm}^{-1}$  and a weak autopeak at approximately  $895\text{ cm}^{-1}$  were observed in the region  $1200\text{--}800\text{ cm}^{-1}$  (Fig. 3b). The absence of the band at  $1033\text{ cm}^{-1}$  can be explained by the overlapping with the band at  $1058\text{ cm}^{-1}$ . Bands at  $1738, 1597, 1510, 1464, 1269, 1205, 855$  and  $805\text{ cm}^{-1}$  showed no or very weak synchronous autopeaks.

The strong synchronous crosspeak  $1698/1664$  was positive, because both peaks changed in the same direction (both increased) (Fig. 3c). The band at  $1698\text{ cm}^{-1}$  corresponded to unconjugated carbonyl groups, possibly due to the side chain oxidation of lignin<sup>11</sup> and carbonyl and carboxylic acid groups formed by free radical attack on cellulose during the biodegradation process<sup>38</sup>. On the other hand, the band at  $1664\text{ cm}^{-1}$  correspond to conjugated carbonyl groups, possibly ortho-quinone structures resulting from the lignin modification by brown rot fungi<sup>39</sup>.

Bands at  $1698$  and  $1664\text{ cm}^{-1}$  show the following crosspeaks in the spectral range of  $1800\text{--}800$ : negative strong synchronous crosspeaks at  $1698/1426, 1698/1371, 1698/1229, 1664/1426, 1664/1371$  and  $1664/1327$ ; negative weak synchronous crosspeaks at  $1698/1464, 1698/1327, 1698/1161, 1698/1108, 1698/1058, 1698/997, 1664/1161, 1664/1108, 1664/1058, 1664/997$  and  $1664/895$  (Fig. 3a, c); positive strong asynchronous crosspeaks at  $1698/1426, 1698/1371, 1698/1327, 1698/1161, 1698/1108$  and  $1698/1058$ ; and positive weak asynchronous crosspeaks at  $1698/1464, 1698/1229$  and  $1698/997$  (Fig. 3d, f).

According to Noda's rule, the bands associated with wood oxidation at  $1698$  and  $1664\text{ cm}^{-1}$  were negatively correlated with bands of polysaccharides:  $1464, 1426, 1371, 1327, 1229, 1161, 1108, 1058$  and  $997\text{ cm}^{-1}$ . While the bands  $1058$  and  $1229\text{ cm}^{-1}$  decreased in intensity with the decrease of the content of residual lignin and holocellulose (Fig. 5), the intensity of band  $1698\text{ cm}^{-1}$  increased with increasing mass loss. This can be explained because the brown rot fungi selectively degraded polysaccharides, causing a decrease in absorbance of the bands associated with these polymers. At the same time, oxidized lignin and carbohydrates increased the absorbance of the bands associated with carbonyl and carboxylic acid groups<sup>1</sup>.

Based on the rule of an asynchronous maps (Fig. 3d-f), the spectral intensity change at  $1698$  and  $1664\text{ cm}^{-1}$  occurred after those at  $1464, 1426, 1371, 1327, 1229, 1161, 1108, 1058$  and  $997\text{ cm}^{-1}$ . This can be explained because the brown rot fungi mainly employ a non-enzymatic oxidative process at the beginning of the degradation process based on the Fenton reaction. The hydroxyl radicals involved are nonselective oxidants that attack all wood components<sup>3</sup>. Polysaccharides are rapidly depolymerised in the early stages of biodegradation<sup>10</sup> producing smaller soluble oligosaccharides or monosaccharides that are used by the fungus in its metabolism<sup>1,11</sup>. In addition, brown rot fungi preferably degrade the S2 layer of the cell wall which contains more polysaccharides<sup>1,40</sup>.

Bands at  $1161, 1108$  and  $1058\text{ cm}^{-1}$  corresponding to polysaccharides showed the following positive strong synchronous crosspeaks with mixed bands corresponding to polysaccharide and lignin at  $1426/1161, 1426/1108, 1426/1058, 1371/1108, 1371/1058, 1327/1108, 1327/1058, 1229/1161, 1229/1108$  and  $1229/1058$  (Fig. 3b, c); and negative strong asynchronous crosspeaks at  $1426/1161, 1426/1108, 1426/1058, 1371/1108, 1371/1058, 1327/1108, 1327/1058, 1229/1161, 1229/1108$  and  $1229/1058$  (Fig. 3e, f). Based on the rule of an asynchronous map, the spectral intensity change at  $1161, 1108$  and  $1058\text{ cm}^{-1}$  occurred before those at  $1464, 1426, 1371, 1327, 1229, 1161, 1108, 1058$  and  $997\text{ cm}^{-1}$ . These bands are highly sensitive to the brown rot fungi biodegradation compared with mixed bands, possibly due to the C-O stretching vibration associated with hemicellulose, which is removed prior to amorphous and crystalline cellulose<sup>1</sup>. Bands at  $1161, 1108$  and  $1058\text{ cm}^{-1}$  did not show asynchronous crosspeaks between them and according to Noda's rule, these bands vary together.

### 3.3 Correlation between standard methods of biodegradation and one dimensional FTIR analysis for wood biodegradation

Decayed wood chips exhibited a progressive weight loss reaching values of  $38.5\%$  after 16 weeks (Fig. 4). At the end of the period of biodegradation the wood progressively turned dark brown and became brittle to the touch, which are typical characteristics of the process of biodegradation by brown rot fungi.

Lignin loss reached values of 5.1% after 16 weeks of incubation. The low value of lignin loss is due to brown rot fungi do not degrade lignin extensively<sup>41-44</sup>. However, lignin is chemically modified<sup>11,45</sup>. In contrast, mass loss of holocellulose reached values of 40.8% after 16 weeks (Fig. 4), which is consistent with the known wood decay pathway of brown rot fungi<sup>1</sup>. The degree of holocellulose depolymerisation is consistent with previous studies that have shown that brown rot fungi rapidly depolymerise holocellulose in the early stages of biodegradation<sup>10</sup>.

Three FTIR bands were selected to verify correlation between standard method of biodegradation and one dimensional FTIR analysis of biodegraded wood chips (Fig. 5). The selected bands were 1698 cm<sup>-1</sup>, associated with the weight loss of wood, 1229 cm<sup>-1</sup>, associated with the lignin loss, and 1058 cm<sup>-1</sup>, associated with the holocellulose loss. The three bands showed high correlation with their respective chemical properties (R>0.85).

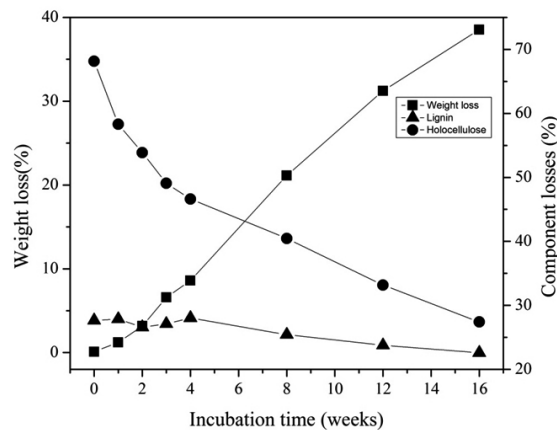


**Figure 4.** Temporal variation of weight loss and components losses of radiate pine wood chips biotreated by *G. trabeum*. Symbols: weight loss (squares), holocellulose (circles), lignin (triangles). Standard deviations from triplicate experiments are smaller than size of symbols.

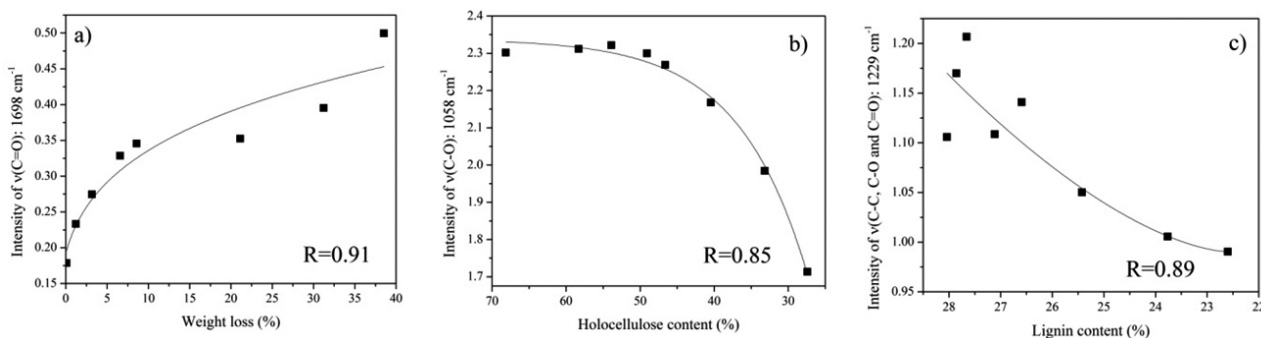


**Figure 5.** Correlation between one dimensional FTIR and chemical properties of biodegraded wood chips (percent of weight loss, total lignin and holocellulose).

#### 4. CONCLUSION

In conclusion, principal component analysis-based two-dimensional correlation FTIR spectroscopy was used to qualitatively characterize the temporal biodegradation of wood by brown rot fungi *G. trabeum*. Bands more sensitive to biodegradation by brown rot fungi were those associated with polysaccharides, as evidenced by the greater extent of intensity changes in absorbance of the bands at 1161, 1108, 1058 and 997 cm<sup>-1</sup>. Oxidation of wood components was observed by changes of intensities in absorbance bands at 1698, associated to carbonyl and carboxylic groups formed from cellulose, and at 1664 cm<sup>-1</sup>, associated with the oxidation of the aliphatic chain of lignin. It was possible to correlate intensity changes of absorbances at the bands 1698, 1229 and 1058 cm<sup>-1</sup> with mass loss, lignin and holocellulose degradation, respectively. The inspection of asynchronous map revealed that wood oxidation began after depolymerization of polysaccharides.

#### ACKNOWLEDGEMENT

This work was supported by FONDECYT 1131101 and FONDECYT 3110094. CIPA Conicyt-Regional R08C1002 and CONICYT (Claudio Pozo PhD fellowship) is gratefully acknowledged.

#### REFERENCES

1. B. Goodell, in Wood Deterioration and Preservation. ACS Symposium Series 845. Brown-rot fungal degradation of wood: our evolving view, B. Goodell et al. eds., Washington DC American Chemical Society, 2003; pp. 97-118.
2. B. Goodell, J. Jellison, J. Liu, G. Daniel, A. Paszczynski, F. Fekete, S. Krishnamurthy, L. Jun, G. Xu, *J. Biotechnol.* **53**, 133, (1997).
3. K. E. Hammel, A. N. Kapich, J. K. A. Jensen, Z. C. Ryan, *Enzyme Microb. Technol.* **30**, 445, (2002).

4. S. M. Hyde, P. M. Wood, *Microbiology* **143**, 259, (1997)
5. K. A. Jensen, Jr., C. J. Houtman, Z. C. Ryan, K. E. Hammel, *Appl. Environ. Microbiol.* **67**, 2705, (2001).
6. Z. Kerem, K. A. Jensen, K. E. Hammel, *FEBS Lett.* **446**, 49, (1999)
7. J. Rodriguez, A. Ferraz, M. P. Mello, in Wood Deterioration and Preservation. ACS Symposium Series 845. Role of metals in wood biodegradation, B. Goodell, et al. eds., Washington DC American Chemical Society, 2003; pp. 154-174.
8. P. M. Wood, *FEMS Microbiol. Rev.* **13**, 313, (1994).
9. B. Goodell, G. Daniel, J. Jellison, Y. Qian, *Holzforchung* **60**, 630, (2006).
10. M. R. Suzuki, C. G. Hunt, C. J. Houtman, Z. D. Dalebroux, K. E. Hammel, *Environ. Microbiol.* **8**, 2214, (2006).
11. T. R. Filley, G. D. Cody, B. Goodell, J. Jellison, C. Noser, A. Ostrofsky, *Org. Geochem.* **33**, 111, (2002).
12. M. Lopretti, D. Cabella, J. Morais, A. Rodrigues, *Process Biochem.* **33**, 657, (1998).
13. V. A. Demin, V. V. Shereshevets, J. B. Monakov, *Russ. Chem. Rev.* **68**, 937, (1999)
14. A. K. Moore, N. L. Owen, *Appl. Spectrosc. Rev.* **36**, 65, (2001)
15. A. Ferraz, J. Baeza, J. Rodriguez, J. Freer, *Bioresour. Technol.* **74**, 201, (2000)
16. K. K. Pandey, *J. Appl. Polym. Sci.* **71**, 1969, (1999)
17. K. K. Pandey, A. J. Pitman, *Int. Biodeterior. Biodegrad.* **52**, 151, (2003)
18. G.-Y. Li, L.-H. Huang, C.-Y. Hse, T.-F. Qin, *Carbohydr. Polym.* **85**, 560, (2011)
19. I. Noda, *Appl. Spectrosc.* **44**, 550, (1990)
20. I. Noda, *Appl. Spectrosc.* **47**, 1329, (1993).
21. I. Noda, *Chin. Chem. Lett.* **26**, 167, (2015).
22. C.-M. Popescu, M.-C. Popescu, C. Vasile, *Microchem. J.* **95**, 377, (2010).
23. I. Noda, *Appl. Spectrosc.* **54**, 994, (2000)
24. Y. M. Jung, H. S. Shin, S. B. Kim, I. Noda, *Appl. Spectrosc.* **56**, 1562, (2002).

25. M. Akhtar, C. Attridge, C. G. Myers, K. T. Kirk, R. A. Blanchette, *Tappi J.* **75**, 105, (1992).
26. D. Harvey Modern analytical chemistry, McGraw-Hill Higher Education a Division of the McGraw-Hill, New York, NY, USA, 2000.
27. C. W. Dence, in *Methods in Lignin Chemistry. The Determination of Lignin*, S. Lin, et al. eds. Springer Berlin, Heidelberg, 1992; pp. 33-61.
28. J. Baeza, J. Freer, in *Wood and cellulosic chemistry. Chemical characterization of wood and its components*, D. N.-S. Hon, et al. eds. Marcel Dekker, Inc., New York, 2001; pp. 275-384.
29. O. Faix, *Holzforschung*, **45**, 21, (1991).
30. K. K. Pandey, A. J. Pitman, *Journal of Polymer Science Part A: Polymer Chemistry*, **42**, 2340, (2004).
31. M. Schwanninger, J. C. Rodrigues, H. Pereira, B. Hinterstoisser, *Vib. Spectrosc.* **36**, 23, (2004).
32. K. Pandey, K. Theagarajan, *Holz Roh Werkst.* **55**, 383, (1997).
33. M. Kacuráková, P. Capek, V. Sasinková, N. Wellner, A. Ebringerová, *Carbohydr. Polym.* **43**, 195, (2000).
34. R. H. Marchessault, *Pure Appl. Chem.* **5**, 107, (1962).
35. K. V. Sarkanen, C. H., E. B., *Tappi J.* **50**, 572, (1967).
36. K. T. Kirk, *Holzforschung*, **29**, 99, (1975).
37. G. Xu, B. Goodell, *J. Biotechnol.* **87**, 43, (2001).
38. T. K. Kirk, R. Ibach, M. D. Mozuch, A. H. Conner, T. L. Highley, *Holzforschung* **45**, 239, (1991).
39. K. Li, X. Geng, *Macromol. Rapid Commun.* **26**, 529, (2005).
40. E. Sjöström *Wood chemistry: Fundamentals and applications*, Academic Press, San Diego, USA, 1993.
41. I. Irbe, I. Andersone, B. Andersons, J. Chirkova, *Int. Biodeterior. Biodegrad.* **47**, 37, (2001).
42. I. Irbe, B. Andersons, J. Chirkova, U. Kallavus, I. Andersone, O. Faix, *Int. Biodeterior. Biodegrad.* **57**, 99, (2006).
43. J. E. Winandy, J. J. Morrell, *Wood Fiber Sci.* **25**, 278, (1992).
44. A. Machuca, A. Ferraz, *Enzyme Microb. Technol.* **29**, 386, (2001).
45. L. Jin, T. P. Schultz, D. D. Nicholas, *Holzforschung* **44**, 133, (1990).